PROCEEDINGS OF SCIENCE

# Comparative study of CTAO medium-size telescopes array layouts performances in gamma-ray burst observations

**D. Cerasole,[1,2,*] A. Acharyya,[3] C. B. Adams,[4] C. Aramo,[5] C. Bartolini,[6,2] W. Benbow,[7] B. Bertucci,[8,9] E. Bissaldi,[1,2] J. H. Buckley,[10] M. Capasso,[11,12] Z. Curtis-Ginsberg,[13] M. De Lucia,[5,14] L. Di Venere,[1,2] M. Escobar Godoy,[15] Q. Feng,[7] E. Fiandrini,[8] N. Giglietto,[1,2] F. Giordano,[1,2] R. Halliday,[16] W. Hanlon,[7] O. Hervet,[15] J. Hoang,[15] W. Jin,[3] D. Kieda,[17] N. La Palombara,[18] E. Leonora,[19] S. Loporchio,[1,2] G. Marsella,[20,21] K. Meagher,[13] R. Mukherjee,[11] N. Otte,[22] F. R. Pantaleo,[1,2] R. Paoletti,[23,24] N. Randazzo,[19] D. Ribeiro,[25] L. Riitano,[13] E. Roache,[7] L. Saha,[7] M. Santander,[3] R. Shang,[11] G. Tripodo,[20,21] V. V. Vassiliev[26] and D. A. Williams[15] for the CTA SCT Project**

[1] *Dipartimento Interateneo di Fisica dell'Università e del Politecnico di Bari, 70126 Bari, Italy*

[2] *INFN Sezione di Bari, 70125 Bari, Italy*

[3] *Department of Physics and Astronomy, University of Alabama, Tuscaloosa, AL 35487, USA*

[4] *Physics Department, Columbia University, New York, NY 10027, USA*

[5] *INFN Sezione di Napoli, 80126 Napoli, Italy*

[6] *Dipartimento di Fisica, Università di Trento, 38123 Trento, Italy*

[7] *Center for Astrophysics | Harvard & Smithsonian, Cambridge, MA 02138, USA*

[8] *INFN Sezione di Perugia, 06123 Perugia, Italy*

[9] *Dipartimento di Fisica e Geologia dell'Università degli Studi di Perugia, 06123 Perugia, Italy*

[10] *Department of Physics, Washington University, St. Louis, MO 63130, USA*

[11] *Department of Physics and Astronomy, Barnard College, Columbia University, NY 10027, USA*

[12] *Broadcom Inc., 2 Wernerwerkstrasse, Regensburg 93049, Germany*

[13] *Department of Physics and Wisconsin IceCube Particle Astrophysics Center, University of Wisconsin, Madison, WI 53706, USA*

[14] *INFN Sezione di Napoli*

[15] *Santa Cruz Institute for Particle Physics and Department of Physics, University of California, Santa Cruz, CA 95064, USA*

[16] *Dept. of Physics, Elmhurst University, Chicago, IL 60126, USA*

[17] *Department of Physics and Astronomy, University of Utah, Salt Lake City, UT 84112, USA*

[18] *INAF - IASF Milano, 20133 Milano, Italy*

[19] *INFN, Sezione di Catania, Via Santa Sofia 64, Catania, 95123 Italy*

[20] *Dipartimento di Fisica e Chimica "E. Segrè", Università degli Studi di Palermo, via delle Scienze, 90128 Palermo, Italy*

[*] Speaker





PoS(ICRC2023)726

[21] *INFN Sezione di Catania, 95123 Catania, Italy*
[22] *School of Physics & Center for Relativistic Astrophysics, Georgia Institute of Technology, Atlanta, GA 30332-0430, USA*
[23] *Dipartimento di Scienze Fisiche, della Terra e dell'Ambiente, Università degli Studi di Siena, 53100 Siena, Italy*
[24] *INFN Sezione di Pisa, 56127 Pisa, Italy*
[25] *School of Physics and Astronomy, University of Minnesota, Minneapolis, MN 55455, USA*
[26] *Department of Physics and Astronomy, University of California, Los Angeles, CA 90095, USA*

*E-mail:* davide.cerasole@ba.infn.it

The Cherenkov Telescope Array Observatory (CTAO), thanks to its unprecedented sensitivity in the very high-energy gamma-ray band for transient phenomena and short-timescale variability, will significantly improve the temporal and spectral characterization of the emission of gamma-ray bursts (GRBs) at the highest energies. The Schwarzschild-Couder Telescope (SCT) is a medium-sized telescope candidate for the CTAO Southern Array endowed with an aplanatic dual-mirror optical system and a compact high-imaging-resolution camera. In this contribution, we aim at quantifying the benefit of adding SCTs to the CTAO-South medium-size array already foreseen in the so-called 'Alpha' configuration through a comparative study of the performances of different layout in GRB observations. We report on the simulation and analysis of GRBs from various medium-size array layouts, adopting burst models based on the detections reported by current instruments at different energies. This study is based on CTA Prod3b simulations with an SCT model dating back to 2016. The results will be updated with a new analysis chain that includes the forthcoming updated SCT model from Prod6 simulations. Furthermore, the event reconstruction used for this analysis is a straightforward extension of the analysis that was optimized for telescopes with larger pixels and coarser image resolution. Continuing improvements in the simulation model and analysis approach might present significant future changes.

38th International Cosmic Ray Conference (ICRC2023)
26 July - 3 August, 2023
Nagoya, Japan

## 1. Introduction

A wide variety of astrophysical sources, both galactic and extragalactic, exhibit emission varying in rapid and unpredictable way across the electromagnetic spectrum over timescales spanning from milliseconds to years. Among these transient sources, GRBs constitute a category rich of outstanding features.

The radiation from GRBs consists primarily of a *prompt* emission peaking in the hard X-ray and soft gamma-ray bands, followed by an *afterglow* emission extending from radio to gamma rays. The prompt phase typically lasts from several milliseconds to hundreds of seconds. During this emission stage, GRBs can become the most luminous sources known in the Universe, liberating as much as $10^{52} - 10^{54}$ erg of isotropic-equivalent energy and manifesting variability on timescales down to sub-millisecond levels [1]. The afterglow emission evolves on longer timescales and it may last up to several months. The burst flux during the afterglow phase can be detected in several energy bands and its temporal evolution is generally described as a power-law decay. The onset of the afterglow radiation is delayed with respect to the prompt emission onset and the afterglow can partially overlap with the prompt stage [2].

GRBs are traditionally classified as short and long bursts depending on whether their prompt phase lasts shorter or longer than 2 s. The progenitors of long-duration bursts are considered to be collapsing massive stars, while short-duration ones are thought to be generated by the coalescence of relativistic compact objects such as neutron star binaries and neutron star-black hole binaries. Thus, GRB investigation represents a probe to the behaviour of matter under the most extreme physical conditions [3]. GRB observations can also be used to probe aspects of cosmic-ray physics and new frontiers in fundamental physics, such as Lorentz invariance violation effects [4].

Imaging Atmospheric Cherenkov Telescopes (IACTs) are ground-based instruments sensitive to gamma rays in the very high-energy (VHE, $E > 100$ GeV) gamma-ray band. A few years ago, a major breakthrough in GRB physics occurred when the current generation of IACTs discovered a VHE component in GRB afterglows. Indeed, the MAGIC observations of GRB 190114C led to the announcement of the detection of TeV emission from a gamma-ray burst during the prompt phase [5], while the H.E.S.S. Collaboration reported the detection of GRB 180720B in the afterglow phase [6]. More recent detections include GRB 190829A by H.E.S.S. [7] and GRB 201216C by MAGIC [8].

The Cherenkov Telescope Array Observatory (CTAO) is the next generation ground-based observatory for gamma-ray astronomy at very high energies and it will employ several tens of telescopes located in two sites, one for each hemisphere, allowing for full-sky coverage. Thanks to its unprecedented sensitivity for transient phenomena and short-timescale variability [9], it will significantly improve the temporal and spectral characterization of the GRB emissions at the highest energies. The Schwarzschild-Couder Telescope (SCT), thanks to its aplanatic dual-mirror optical system and compact camera equipped with silicon photomultipliers (SiPMs), is designed to reach an optical point spread function (PSF) of 3.2 arcmin over a wide field-of-view (FoV) of 8°. In this contribution, we aim at quantifying the benefit of adding SCTs to the CTAO-South medium-size array foreseen in the so-called 'Alpha' configuration through a comparative study of the performance of different layouts in GRB observations.

**Figure 1:** The pSCT at the Whipple Observatory in Arizona.

## 2. Schwarzschild-Couder Telescope and CTAO-South medium-size array layouts

In order to provide a wide energy coverage from tens of GeV to hundreds of TeV, CTAO will operate three different telescope types, referred to as Large, Medium and Small-Sized Telescopes (LSTs, MSTs and SSTs, respectively), each one optimized in a specific energy range. The MSTs are designed to provide sensitivity in the core of the CTAO energy range, from hundreds of GeV to tens of TeV.

The baseline design for the MSTs employs a single-reflector optics with Davies-Cotton (DC) geometry and a camera equipped with approximately 2000 photomultiplier tubes (PMTs). The SCT represents a candidate MST for CTAO characterized by a 9.7 m aperture dual-mirror optical system in Schwarzschild–Couder design for a simultaneous correction of spherical and comatic aberrations over the whole 8° FoV. The SCT is equipped with a 0.8 m diameter camera with 11328 SiPMs. Such refined optics and fine pixelization yield better event reconstruction, improved background suppression and angular resolution with respect to current IACTs. A prototype SCT (pSCT) has been constructed at the Fred Lawrence Whipple Observatory in Arizona, USA, shown in Figure 1. In the first campaign of observations with the pSCT, VHE gamma-ray emission from the Crab Nebula was successfully detected, hence establishing proof of concept of the SCT design [10].

The CTAO Southern Array site will be based in Paranal, Chile. In the foreseen 'Alpha' configuration for CTAO-South, the medium-size array comprises 14 MSTs in the F4 layout, shown in the left panel of Figure 2, while the small-size array consists in 37 SSTs, with a total area of $\sim$ 3 km$^2$ covered by the array of telescopes. In this work, we focus only on the medium-size subarray performance. The layouts resulting from adding 11 MSTs or 11 SCTs to the F4 layout are in the mid and right panels, respectively, and they are referred to as the C0 and M2 layouts. The

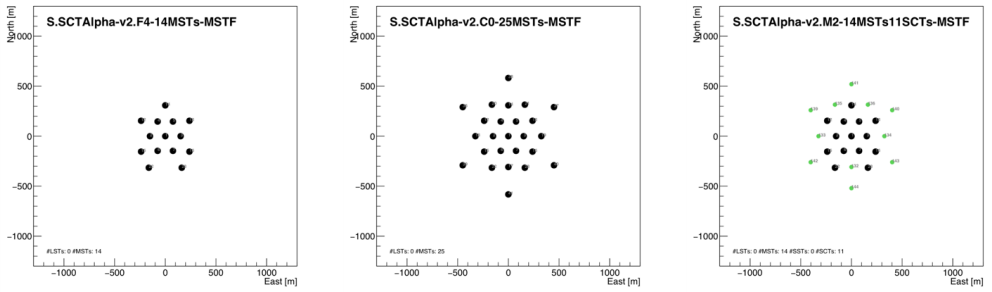


**Figure 2:** CTAO-South medium-size array layouts considered in the gamma-ray burst simulations. In the left panel, the F4 layout with 14 MSTs in DC design foreseen in the CTAO 'Alpha' Configuration. In the mid (right) panel, the C0 (M2) layout resulting from adding 11 DC-MSTs (SCTs) to the F4 layout.

performances of these layouts, e.g. in terms of effective area and angular resolution, are described in their Instrument Response Functions (IRFs), which derive from simulations of extensive air showers in the atmosphere and Cherenkov light production and propagation via the CORSIKA code [11], simulations of the detector response through the `sim_telarray` package [12] and reconstruction of the Cherenkov images using the Eventdisplay analysis software package [13]. High-level simulation and analysis packages employ the IRFs to generate candidate gamma-ray event lists and to evaluate science data products such as skymaps, light-curves and spectra.

We chose to simulate and analyse high-level observational data from the three previously mentioned layouts to quantify the improvement that can be reached adding the SCTs to the CTAO-South medium size array in transient observations. For similar simulation studies on observations of steady Galactic extended sources, the reader is addressed to [14].

## 3. GRB simulations and analysis pipeline

Simulations and analyses of observational data were carried out by means of a pipeline based on the `ctools` package [15]. We used the prod3b [16] multiplicity-2 IRFs optimized for half-hour observations at 20° zenith angle. The adopted simulation and analysis energy range extended from 200 GeV to 10 TeV. To account for the residual isotropic background which originates mainly from showers initiated by charged cosmic-rays, CTAIrfBackground[1] was included both in the simulation and analysis procedures.

We decided to simulate and analyse data from three historical GRBs observed at VHE by IACTs, i.e. GRB 190114C, GRB 180720B and GRB 190829A, following a purely phenomenological approach. As burst models, we adopted the ones reported in the papers by the MAGIC and H.E.S.S. Collaborations that described the burst detections [5–7]. As the intrinsic spectra of all three GRBs were well fitted with power-law models and for none of them was there significant evidence of evolution of the spectral index with time, we modeled the spectral model component with power-laws of the form $F(E) \propto N_0(E/E_0)^{-\gamma}$ with constant spectral index. We considered the bursts as point-like sources. In the adopted models, we considered an afterglow-only VHE burst emission, with no prompt contribution in the energy band of interest. The temporal evolution of the bursts

[1] http://cta.irap.omp.eu/ctools/users/user_manual/models_bgd_iact.html

was assumed to be a power law $F(t) \propto (t/t_0)^{-\alpha}$ with the constant decay indices $\alpha$ reported in the corresponding reference papers. Finally, to account for the effects of the EBL attenuation of gamma rays through their path across cosmological distances, the GRB intrinsic models were folded with EBL-extinction terms based on the Dominguez et al. model [17].

For each burst, we performed simulations and analyses of data from a sky region centered on the burst position and with 4° radius in several time windows. For each time interval, a binned maximum-likelihood fit was performed dividing the energy range to 24 bins and the angular coordinates space to pixels with size of 0.02°. In the fit procedures, the spectral and spatial parameters of the GRB were left free, as well as the background normalization.

To check that the constructed simulation and analysis pipeline was working properly, data were simulated and analysed in the same time windows as the spectral energy distributions (SEDs) reported in the reference papers. The best-fit models and reconstructed SEDs proved to be compatible with the ones observed by MAGIC and H.E.S.S., thus ensuring the pipeline effectiveness.

## 4. Comparison of performances in gamma-ray burst observations

The performance comparison study was carried out simulating and analysing 1 hour of data starting from different $T_{start}$ times, from $T_0 + 60$ s at 1-hour steps, using the procedure described above. The top panel of Figure 3 reports the TS values[2] for the GRB detection obtained with the three layouts for each of these analyses at different $T_{start}$ times for GRB 190114C, as a function of $T_{start}$. Two figures of merit to quantify the improvement in adding the SCTs were highlighted.

We considered the ratios of the TS values obtained with the various layouts as first characteristic figure of merit. The values of TS(C0)/TS(F4) and TS(M2)/TS(F4), plotted in the mid panel of Figure 3, have average values of roughly 1.9 and 2.4, respectively. This indicates that the statistics gathered with the M2 layout are richer than for the other two layouts.

The TS vs $T_{start}$ curves were fitted with the function

$$TS(T_{start}) = A\left[(T_{start}+1)^{1-\alpha} - (T_{start})^{1-\alpha}\right]^2, \quad (1)$$

with $T_{start}$ values expressed in hours, which derives from an approximate evaluation of the TS in 1-hour observations, starting at $T_{start}$, of a source whose flux decays in time as $F(t) \propto (t/t_0)^{-\alpha}$. The $T_{start}$ values at which these curves intercepted $TS = 25$ were extrapolated. $T_{start,max}$ is defined as the maximum delay, with respect to the burst trigger time, with which a 1-hour observation can give a 5 sigma detection level. The $T_{start,max}$ values for simulated GRB 190114C observations with the F4, C0 and M2 layouts are respectively 5, 7 and 8 hours, thus the M2 value is 1.6 times higher than the F4 value and 1.1 greater than the C0 value. We adopted the ratios of the $T_{start,max}$ values for the three layouts as a figure of merit to characterize their comparison.

Analogous improvements were found applying this procedure to GRB 180720B and GRB 190829A. The results are summarized in Table 1.

From the simulations and analyses of the three historical GRBs observed at VHE gamma rays, we find that, on average, given the same observational conditions, the TS values obtained with the

[2]Given $\bar{L}$ and $\bar{L}_0$ the maximum-likelihood values of the model that includes the burst and a background-only model, respectively, the TS can be defined as TS = $2(\log \bar{L} - \log \bar{L}_0)$.

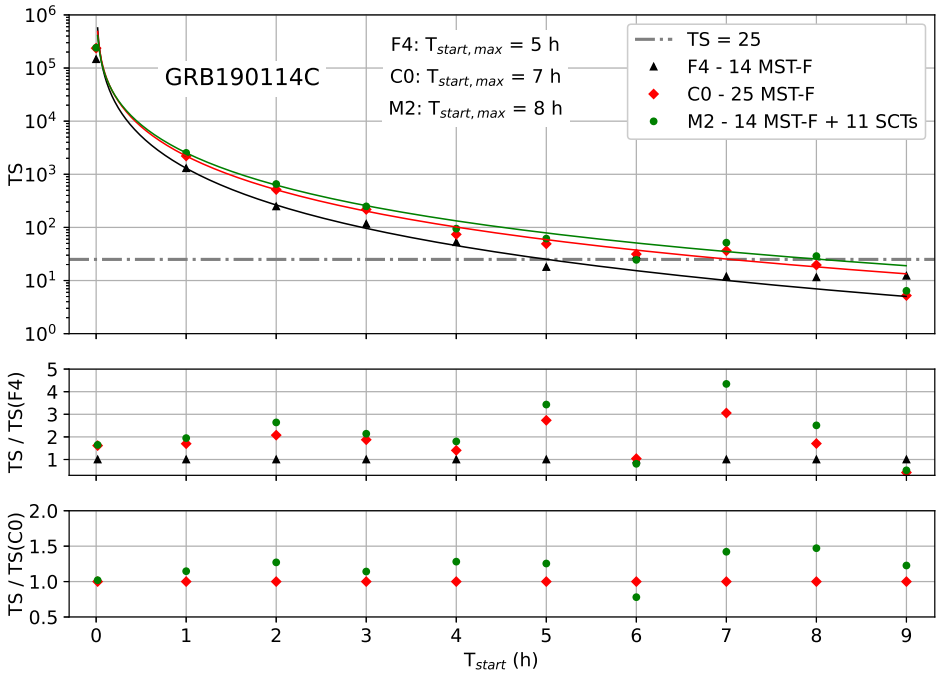


**Figure 3:** In the top panel, TS values resulting from the analyses of 1-hour GRB 190114C observations at different $T_{start}$, from $T_0 + 60$ s, for the three layouts of interest. In the mid and bottom panels the TS values normalized to F4 and C0, respectively.

**Table 1:** Average TS ratios in 1-hour analyses and $T_{start,max}$ values for the three layouts resulting from the simulations of GRB 190114C, GRB180720B and GRB 190829A.

| | GRB 190114C | GRB 180720B | GRB 190829A |
|---|---|---|---|
| ⟨TS(C0)/TS(F4)⟩ | 1.9 | 1.8 | 2 |
| ⟨TS(M2)/TS(F4)⟩ | 2.4 | 2.2 | 2.6 |
| ⟨TS(M2)/TS(C0)⟩ | 1.2 | 1.2 | 1.3 |
| $T_{start,max}(F4)$ | 5 h | 20 h | 41 h |
| $T_{start,max}(C0)$ | 7 h | 27 h | 67 h |
| $T_{start,max}(M2)$ | 8 h | 31 h | 77 h |

M2 layout are larger than F4 ones by a factor 2 at least and, also, larger than C0 TS values by roughly 20%, while the latest delays that allow detection with 1-hour integration times with the M2 layout are approximately a factor 2 larger than the F4 ones and greater than the respective C0 values.

## 5. Conclusions

The pipeline we implemented allowed us to quantify the improvement that could be reached by adding the SCTs to the CTAO-South medium-size array, through two figures of merit. The higher TS

values obtained with the layout which includes the SCTs represent the increase in gathered statistics, and also the better characterization of the VHE emission properties of the observed transient event. The higher $T_{start,max}$ times with the SCT-enriched layout represent the greater chances to detect a burst if the observation starts after a certain time from the burst trigger. This parameter holds particular importance for IACTs, as their duty cycle is $\approx 10\%$, hence the larger $T_{start,max}$ values express the enhancement of the possibility to detect fast transient events even if they happen during daytime.

The results presented in this contribution assumed observations at fixed 20° zenith angle. More refined studies taking into account the variations in altitude and azimuth of the GRB and relying on a richer population of bursts are foreseen among the future steps.

## Acknowledgments

This research has made use of the CTA instrument response functions provided by the CTA Consortium and Observatory, see www.cta-observatory.org/science/ctao-performance/ for more details. Furthermore, we would like to thank the computing centres that provided resources for the generation of the Instrument Response Functions, see [18] for a complete list.

We gratefully acknowledge financial support from the agencies and organizations at www.cta-observatory.org/consortium_acknowledgments/.

## References

[1] Mészáros P., Gamma-ray bursts, 2006, *Rep. Prog. Phys.* **69** 2259

[2] Miceli D., Nava L., Gamma-Ray Bursts Afterglow Physics and the VHE Domain, *Galaxies* **2022** 10(3) 66

[3] Abbott B. P. et al., Multi-messenger Observations of a Binary Neutron Star Merger, 2017, *ApJL* **848** L12

[4] Acciari V. A. et al., Bounds on Lorentz Invariance Violation from MAGIC Observation of GRB 190114C, 2020, *Phys. Rev. Lett.* **125** 021301.

[5] Acciari V. A. et al., Teraelectronvolt emission from the $\gamma$-ray burst GRB 190114C, 2019, *Nature* **575** 455

[6] Abdalla H. et al., A very-high-energy component deep in the $\gamma$-ray burst afterglow, 2019, *Nature* **575** 464

[7] Abdalla H. et al., Revealing x-ray and gamma ray temporal and spectral similarities in the GRB 190829A afterglow, 2021, *Science* **372** 1081

[8] Fukami S. et al., Very-high-energy gamma-ray emission from GRB 201216C detected by MAGIC, 2022, *PoS* ICRC2021 788

[9] Funk S. et al., Comparison of Fermi-LAT and CTA in the region between 10–100 GeV, 2013, *APh* **43** 348

[10] Adams C. B. et al., Detection of the Crab Nebula with the 9.7 m prototype Schwarzschild-Couder telescope, 2021, *APh* **128** 102562.

[11] Heck, D., Knapp, J., Capdevielle, J. N., Schatz, G., Thouw, T., CORSIKA: A Monte Carlo Code to Simulate Extensive Air Showers, 1998, Report FZKA 6019

[12] Bernlöhr K., Simulation of Imaging Atmospheric Cherenkov Telescopes with CORSIKA and sim_telarray, 2008, *APh* **30** 149

[13] Maier G., Holder J., Eventdisplay: An Analysis and Reconstruction Package for Ground-based Gamma-ray Astronomy, 2018, *PoS* ICRC2021 747

[14] R.Shang et al., The optics and camera system of the Schwarzschild-Couder Telescope and the performance improvement to the CTA, 2023, *These proceedings*

[15] Knödlseder J. et al., GammaLib and ctools: A software framework for the analysis of astronomical gamma-ray data, 2016, *A&A* **593** A1

[16] Bernlöhr K., Maier G., Moralejo A. (2022). CTAO Simulation Telescope Models for CORSIKA and sim_telarray - prod3b (1.0.0) [Data set]. Zenodo. https://doi.org/10.5281/zenodo.6219128

[17] Domínguez A. et al., Extragalactic background light inferred from AEGIS galaxy-SED-type fractions, 2011, *MNRAS* **410** 2556

[18] Cherenkov Telescope Array Observatory, Cherenkov Telescope Array Consortium. (2016). CTAO Instrument Response Functions - version prod3b-v2 (prod3b-v2/v1.0.0) [Data set]. Zenodo. https://doi.org/10.5281/zenodo.5163273